

On creation and evolution of dark solitons in Bose-Einstein condensates

V.A. Brazhnyi^{1,*}, A.M. Kamchatnov^{1,2,†} and V.V. Konotop^{1‡}

¹*Centro de Física da Matéria Condensada, Universidade de Lisboa,*

Complexo Interdisciplinar, Av. Prof. Gama Pinto 2, Lisboa 1649-003, Portugal

²*Institute of Spectroscopy, Russian Academy of Sciences, Troitsk 142190, Moscow Region, Russia*

Generation of dark solitons from large initial excitations and their evolution in a quasi-one-dimensional Bose-Einstein condensate trapped by a harmonic potential is studied analytically and numerically. In the case of a single deep soliton main characteristics of its motion such as a frequency and amplitude of oscillations are calculated by means of the perturbation theory which in the leading order results in a Newtonian dynamics, corrections to which are computed as well. It is shown that long-time dynamics of a dark soliton in a generic situation deviates substantially from outcomes of the naive application of the Ehrenfest theorem. We also consider three different techniques of controllable creation of multi-soliton structures (soliton trains) from large initial excitations and calculate their initial parameters (depths and velocities) with the use of a generalized Bohr-Sommerfeld quantization rule. Multi-soliton effects are discussed.

PACS numbers: 03.75.Lm, 03.75.Kk, 05.45.Yv

I. INTRODUCTION

Experimental observations of dark solitons in a cigar-shaped Bose-Einstein condensate (BEC) of sodium [1] and of ⁸⁷Rb [2] atoms and in a near spherical BEC of ²³Na atoms [3] have stimulated intensive theoretical studies devoted to generation and evolution of such excitations in BEC's. At low enough temperature the condensate evolution is described sufficiently well by the Gross-Pitaevskii (GP) equation [4], which is originally three-dimensional (3D) but in some cases is reducible to a 1D nonlinear Schrödinger (NLS) equation with an external potential. As such cases we can mention a BEC with a “pancake” geometry (see e.g. [5]) and a low-density BEC in a “cigar-shape” trap (see e.g. [6]). If the respective size of the condensate is much bigger than the characteristic dimension of an excitation in it, then it is commonly believed that the conventional (i.e. without potential) NLS equation can be used for understanding the excitation evolution during initial intervals of time. Such approximation was used for description of dark soliton dynamics in quasi-1D BEC with a positive scattering length (see e.g. [7]). If, however, a size of an excitation is comparable with the size of the condensate or if one is interested in long-time dynamics, then influence of a trap potential must be taken into account. This is especially important in the case of dark solitons. One of the physical reasons for that is that in the presence of a trap potential the BEC density becomes a function of a space coordinate and/or time. From the mathematical point of view it means that the trap potential changes boundary conditions for the macroscopic wave function of the condensate at the infinity. (Note that this does

not happen in the case of bright solitons in a BEC with negative scattering length, which in a quasi-1D case were recently observed experimentally [8]).

In the homogeneous NLS equation, which is exactly integrable [9], the long-time evolution of an excitation can be reduced to the motion of a set of solitons and to propagation of linear waves. Solitons in that case are well defined objects and their parameters can be found by means of the inverse scattering transform method [9]. In particular, constant velocities of solitons (as well as other soliton parameters) can be calculated from the associated linear spectral problem using the initial distribution of the macroscopic wave function. In the presence of a trap this method cannot be applied without some reservations. Moreover, a dark soliton against a nonuniform background is not a well defined object anymore. Therefore separation of the excitation evolution into “soliton part” and “background part” is somewhat conditional. Even if such separation is meaningful at the initial moment of time, during propagation soliton parameters become functions of time. In particular, a change of a soliton shape can be so dramatic that the distinction between the soliton and the background may lose its sense and must be reconsidered. Then one meets a problem of long-time description of the soliton evolution. This problem becomes even more complicated in the case when an initial excitation results in formation of many solitons (soliton trains). Thus, one of the aims of the present paper is to consider evolution of excitations which initially can be classified as one- and multi-soliton ones in 1D BEC confined by a harmonic potential.

Several aspects of this problem have already been addressed in literature. In particular, there have been reported several evidences that the dynamics of a dark soliton or a few solitons in a BEC trapped in a harmonic potential is oscillatory [10, 11, 12, 13]. In one of the first publications [10] it has been suggested that for description of the dark soliton evolution one can employ the Ehrenfest theorem which allows one to define

*Electronic address: brazhnyi@cii.fc.ul.pt

†Electronic address: kamch@isan.troitsk.ru

‡Electronic address: konotop@cii.fc.ul.pt

a frequency of oscillations, and on this basis an empiric formula $m\ddot{x} = -\partial U/\partial x$, where $U(x)$ is a trap potential, for Newtonian dynamics of a dark soliton has been proposed (although a definition for the coordinate of a dark soliton x has not been given). A similar equation for a dark soliton motion against a background was derived in [12] by means of the multi-scale analysis. In numerical simulations provided in [13] authors observed an oscillatory behavior of small amplitude dark solitons. That paper however has left open a question about the frequency of the oscillations and their amplitude. Also, although an important question about a choice of a particular form of the background has been posed (since a “wrong” choice results in rapidly growing oscillations of the background), it has been solved by numerical means on the basis of elimination of the mentioned oscillations of the background, leaving analytical fundamentals for such a choice open, as well. Moreover in Ref. [13] it has been found that the amplitude of a small-depth dark soliton increases as the soliton approaches a turning point, which does not corroborate with the previous findings [10, 11, 12] where it was reported that the shape of a dark soliton is preserved during propagation against a background. Finally, it is worthwhile to mention that in Refs. [10, 11, 12, 13] one can find no information about long-time behavior of a dark soliton in a trap potential.

Another related issue of the theory is generation of dark solitons. The discussion in the literature has been mainly concerned with such methods as laser induced Raman transition between two internal states of the condensate [14], “phase imprinting” [2, 15], modulational instability [6], and the use collision of two initially separated condensates [10, 11].

In Ref. [10] it was supposed that generation of the dark solitons with different initial velocities can be achieved in a collision of two pieces of initially displaced condensates. By numerical calculations it was shown that in the presence of a trap all solitons have essentially the same classical period of oscillations given by harmonic classical dynamics. The same mechanism of generation of the multi-soliton structures was considered in Ref. [11] (although a number of the generated solitons and their initial parameters were not calculated). In Ref. [14] a scheme to create dark solitons in a BEC with the use of coherent Raman process which couples internal atomic levels of the condensate with a laser was proposed. In a recent work on the controlled generation of dark solitons by phase imprinting method [15] the authors provided a simple theoretical description of the creation of the dark solitons in the experiment [2]. Considering a very short time scale, they neglected the trap potential, and in this case for a given initial phase step, a number of solitons and their initial velocities were calculated analytically by mapping Zakharov-Shabat eigenvalue problem into the pendulum problem, which is mathematically much simpler.

Thus, the second aim of the present paper is the study of generation of multi-soliton structures from an arbitrary

initial excitation in a nonuniform condensate confined by a harmonic potential as well as their evolution.

The organization of the paper is as follows. In Section II the dynamics of a single dark soliton in a harmonic trap potential is considered in detail. First of all we argue the choice of the analytical form of the background which is necessary for a stable long-time dynamics of a soliton making it nearly integrable. We show also that one can define two characteristic coordinates associated with the dark soliton: a position of the center of mass (the mass being negative) and a position of a local minimum of the intensity. The both values being the same in the case of a homogeneous background display different behavior subject to the effect of the potential. The first one is governed by the Ehrenfest theorem while another one can be described on the basis of the perturbation theory of solitons [16]. Theoretical predictions are compared with the numerical simulations. Non-adiabatic effects of the soliton dynamics and the behavior of its phase are discussed. In Section III we describe generation of soliton trains in a trapped BEC from initial excitations of different types and study their evolution. In the case of perturbation of the condensate density by a large and smooth initial pulse we find initial parameters of created solitons with the use of generalized Bohr-Sommerfeld quantization rule [17]. Using the results of Section II we predict locations of turning points which are well confirmed by direct numerical simulations. We also discuss behavior of dark solitons generated by the phase imprinting method and creation of solitons during collisions of two condensates in the presence of the harmonic trap potential. The outcomes of the theory are summarized in Conclusion. For the sake of convenience a summary of some technical results of the perturbation theory for dark solitons is given in the Appendix.

II. MOTION OF A SINGLE DARK SOLITON IN A PARABOLIC TRAP

A. Statement of the problem

As it is customary, we start with the GP equation for the order parameter $\psi \equiv \psi(\mathbf{r}, t)$:

$$i\hbar \frac{\partial \psi}{\partial t} = -\frac{\hbar^2}{2m} \Delta \psi + V_{trap}(\mathbf{r})\psi + g_0 |\psi|^2 \psi, \quad (1)$$

where we use the standard notations: $g_0 = 4\pi\hbar^2 a_s/m$, a_s being the s -wave scattering length, which is considered positive, and m being the atomic mass; $V_{trap}(\mathbf{r})$ is a trap potential.

A self-consistent reduction of Eq. (1) to a 1D NLS equation can be made in various situations (see e.g. [5, 6]).

(i) In the case of a pancake BEC we suppose that in the transverse direction (i.e. in the direction orthogonal to the x -axis) the size of the condensate is large enough to be considered infinite in the first approximation. This leads

to the trap potential of the form $V_{trap} = \frac{m}{2}\omega_0^2 x^2$ where ω_0 is the harmonic oscillator frequency. Then, in order to rewrite the dynamical equation in a dimensionless form we make a substitution

$$\psi(\mathbf{r}, t) = 2^{\frac{1}{4}}(4\pi\nu a_s a_0^2)^{-\frac{1}{2}} \exp\left(i\mathbf{k}_\perp \mathbf{r}_\perp - i\frac{\hbar k_\perp^2}{2m}t\right) \Psi(x, t), \quad (2)$$

where $\mathbf{r}_\perp = (y, z)$ and $a_0^2 = \frac{\hbar}{m\omega_0}$, and make a change of independent variables $x \mapsto \nu^{1/2}a_0 x/2^{1/4}$, $t \mapsto 2^{1/2}\nu t/\omega_0$, which results in the canonical form of the NLS equation with a parabolic potential

$$i\frac{\partial\Psi}{\partial t} + \frac{\partial^2\Psi}{\partial x^2} - 2|\Psi|^2\Psi = \frac{1}{2}\nu^2 x^2\Psi \quad (3)$$

(in what follows Ψ is also referred to as a macroscopic wave function). Notice that in contrast to the generally accepted renormalization, here we introduced a parameter ν which on the one hand characterizes a strength of the parabolic potential in dimensionless equation (3), and on the other hand is connected with the density of particles in the condensate. To elucidate this connection, we note that the condensate wave function $\Psi(x, t)$ is normalized according to

$$\int_{-\infty}^{\infty} |\Psi(x, t)|^2 dx = 4\pi 2^{-1/4} \nu^{1/2} a_s a_0 n_0, \quad (4)$$

where n_0 stands for the ‘‘transverse density’’ of particle, i.e. $n_0 = \mathcal{N}/S$, \mathcal{N} is the total number of particles and S is the area of the transverse cross section of the condensate. (Formally one has to consider the ‘‘thermodynamical’’ limit $\mathcal{N} \rightarrow \infty$, $S \rightarrow \infty$ at $n_0 = \text{const.}$)

On the other hand let us consider an unperturbed condensate wave function $\Psi(x, t) = \exp(-i\mu t)\Psi(x)$ (μ is a renormalized chemical potential) which solves the stationary equation

$$\begin{aligned} \frac{d^2\Psi}{dx^2} + \mu\Psi - 2|\Psi|^2\Psi &= \frac{1}{2}\nu^2 x^2\Psi, \\ \Psi(0) &= 1, \quad \Psi'(0) = 0. \end{aligned} \quad (5)$$

This is clear that Ψ decays exponentially at $|x| \rightarrow \infty$, and thus one can expect that

$$\int_{-\infty}^{\infty} |\Psi(x)|^2 dx \simeq \int_{-\sqrt{2\mu}/\nu}^{\sqrt{2\mu}/\nu} |\Psi_{TF}(x)|^2 dx = \frac{(2\mu)^{3/2}}{3\nu} \quad (6)$$

where

$$\Psi_{TF}(x) = \frac{1}{2} \sqrt{2\mu - \nu^2 x^2} \quad (7)$$

is the condensate wave function in the Thomas-Fermi approximation and $\mu \simeq 2$ for $\nu \ll 1$. More careful numerical study of Eq. (5) gives corrections to (6)

$$\int_{-\infty}^{\infty} |\Psi(x)|^2 dx = \frac{C(\nu)}{\nu}, \quad (8)$$

where $C(\nu)$ is a very slow function of ν equal to $C(\nu) \simeq 2.67$ with accuracy better than 1% in the interval $0.1 \leq \nu \leq 0.3$. Comparison of Eqs. (4) and (8) shows that

$$\nu \simeq \left(\frac{2.67 \cdot 2^{1/4}}{4\pi}\right)^{2/3} \frac{1}{(a_s a_0 n_0)^{2/3}} \simeq \frac{0.4}{(a_s a_0 n_0)^{2/3}}. \quad (9)$$

This formula determines ν in terms of the physical parameters of the system under consideration. As an example one can consider $\mathcal{N} = 10^5$ atoms of ^{87}Rb ($a_s \approx 5.8 \text{ nm}$) condensed in a trap with $a_0 \approx 1 \mu\text{m}$ (what corresponds to the frequency $\omega_0 \sim 7 \cdot 10^2 \text{ Hz}$) and with transverse radius $\approx 14 \mu\text{m}$. Then we get $\nu \approx 0.2$. As it is evident, increasing of the density by a factor 10 results in decreasing of the small parameter by approximately the same factor.

Thus, ν can be viewed as a natural small parameter of the problem and therefore in what follows we shall consider the case $\nu \ll 1$.

In order to construct the theory yet another condition is to be imposed: the longitudinal dimension of the condensate $\sim \nu^{-1}$ must be sufficiently large compared with a characteristic width $l \sim 1$ of a typical soliton solution. Then it makes sense to speak about a soliton against an inhomogeneous background. More specifically, we require $l/a_0 \sim \sqrt{\nu}$. This however is not a strong restriction since already at $\nu \approx 0.1$ the relation $l \approx a_0/3$ (which corresponds to the actual experimental settings) is verified.

(ii) Considering a cigar-shaped BEC one uses the multi-scale expansion (see e.g. [6] for details) with respect to the small parameter $\epsilon = 8\pi\mathcal{N}a_s a_\perp/a_0^2 \ll 1$ (it can be viewed as smallness of the energy of two-body interaction compared with the kinetic energy) where $a_\perp = (\hbar/m\nu_\perp)^{1/2}$ is the linear oscillator length in the transverse direction and ν_\perp is the linear oscillator frequency in the transverse direction. The smallness of the parameter ϵ provides the conditions when the consideration can be restricted by the lowest mode in the three-dimensional parabolic trap: at larger ϵ interactions of modes become essential and must be taken into account what leads to a set of coupled nonlinear Schrödinger equations. In this case the time is measured in units $2/\nu_\perp$ and spatial coordinate along the cigar axis is measured in units a_\perp . The parameter ν is now defined as $\nu = a_\perp/a_0$ and can be easily made as small as necessary. Meantime, in that case one has to verify the condition $\epsilon \ll 1$ necessary for applicability of the theory developed below. Let us do that for the data analogous to ones reported in [1] imposing however a lower particle density, i.e. considering a BEC of $\mathcal{N} = 5 \cdot 10^5$ sodium atoms ($a_s \approx 2.7 \text{ nm}$). Then for $a_0 \approx 450 \mu\text{m}$ and $a_\perp \approx 10 \mu\text{m}$ one estimates $\nu \approx 0.1$. Thus in the case at hand the limit of small effective parameter ν is also reachable for available experimental settings.

In order to complete the statement of the problem we have to specify the terminology ‘‘long-time’’ dynamics. We will do this for a pancake geometry. A unity of time, $\Delta t = 1$, in the dimensionless variables corresponds to

ω_0/ν real seconds. This means, for example, that considering a BEC of ^{87}Rb atoms in a trap with the longitudinal size of order of $a_0 \sim 1\mu\text{m}$ and assuming that $l/a_0 \sim 0.3$, a unity of the dimensionless time will correspond to 0.18 ms. A typical life-time of a BEC reachable in today experiments can be estimated as at least 50 ms, which means that it is meaningful (in a BEC context) to investigate the dynamics of the excitations for times at least up to 300 dimensionless units. As one expects ν to be of order of the frequency of soliton oscillations in a trap, the above estimate corresponds to approximately 20 periods of oscillations. Thus, long-time dynamics in the present paper is understood as a dynamics displaying more than 10 oscillations.

B. Choice of the background and near-integrable dynamics

When $\nu = 0$, Eq. (3) reduces to the conventional NLS equation which admits a stable constant-background solution $|\Psi(x, t)|^2 = \rho_0 (= \text{const})$, against which one can construct a dark soliton solution [9]

$$\Psi_s(x, t) \equiv \sqrt{\rho_0} \frac{1 + e^{i\vartheta} \exp\{\eta_0[x - X(t)]\}}{1 + \exp\{\eta_0[x - X(t)]\}}. \quad (10)$$

Here $X(t) = Vt + X_0$, $V = -2\sqrt{\rho_0} \cos(\vartheta/2)$ and $\eta_0 = 2\sqrt{\rho_0} \sin(\vartheta/2)$ are the soliton coordinate, velocity, and width, respectively. X_0 is the coordinate at initial moment of time. Due to the symmetry of the problem, the parameter ϑ which characterizes the phase difference of $\Psi_s(x, t)$ at $\pm\infty$ can be restricted to the interval $0 \leq \vartheta \leq \pi$. For $\vartheta = \pi$ the BEC density vanishes at the soliton center and in this case a soliton is often called “black” while for other ϑ a soliton is referred to as “grey”. The limit $\vartheta \ll 1$ corresponds to small amplitude solitons.

When the trap potential is switched on, the function $\Psi_s(x, t)$ given by (10) is not a solution of (3) anymore. However, one could expect that if a region of soliton localization is much less than the size of the background, i.e. when $\nu \ll \eta_0$, and if in the vicinity of the potential center the initial condition for Eq. (3) is chosen to be close enough to the dark soliton one, then a solution of Eq. (3) can be searched in a form of a “dark soliton” $\Phi(x, t)$ against an inhomogeneous background $F(x)$, i.e. in the form

$$\Psi(x, t) = F(x) \cdot \Phi(x, t), \quad (11)$$

where $\Phi(x, 0) = \Psi_s(x, 0)$, $\Psi_s(x, t)$ being given by (10).

Ansatz (11) is meaningful if the dynamics of $\Phi(x, t)$ is close, in some sense, to the dynamics of $\Psi_s(x, t)$. Since $\Psi_s(x, t)$ is governed by the unperturbed (i.e. with $\nu = 0$) NLS equation, to satisfy the last requirement it is natural to choose $F(x)$ such that the resulting equation for $\Phi(x, t)$ would be close to the NLS equation. This can be

achieved by requiring $F(x)$ to be an eigenfunction of the nonlinear spectral problem [c.f. (5)]

$$F_{xx} + \left(\omega_b - \frac{(\nu x)^2}{2} \right) F - 2\rho_0 F^3 = 0, \quad (12)$$

$$\lim_{x \rightarrow \pm\infty} F(x) = 0, \quad (13)$$

which satisfies the following normalization conditions

$$F(0) = 1, \quad F_x(0) = 0. \quad (14)$$

In (12) ω_b is an eigenvalue.

Indeed, substituting ansatz (11) in Eq. (3), one obtains

$$i\Phi_t + \Phi_{xx} - 2(|\Phi|^2 - \rho_0)\Phi = R[\Phi, F], \quad (15)$$

where

$$R[\Phi, F] \equiv -2(\ln F)_x \Phi_x + 2\Phi(|\Phi|^2 - \rho_0)(|F|^2 - 1). \quad (16)$$

Next, one can estimate the order of magnitude of $R[\Phi, F]$ considering $x\nu$ small enough:

$$\begin{aligned} (\ln F)_x &\sim \nu^2 x, & \Phi_x &\sim \eta, \\ (|\Phi|^2 - \rho_0)(|F|^2 - 1) &\sim \nu^2 \eta^2 x^2, \end{aligned} \quad (17)$$

where it is taken into account that in a vicinity of the center of the potential, i.e. at $x\nu \ll 1$, $F(x)$ can be expanded in the Taylor series

$$F(x) = 1 + \frac{2\rho_0 - \omega_b}{2} x^2 + O(x^4). \quad (18)$$

Substitution of (18) into (12) with subsequent expansion in powers of “small” x (i.e. $x = o(\nu^{-1})$) and small ν yields the estimate for the eigenvalue

$$\omega_b = 2\rho_0 + \frac{\nu^2}{4\rho_0} + O(\nu^4). \quad (19)$$

As it follows from the definition of the soliton width, we have $\eta = O(1)$ whenever $\rho_0 = O(1)$. This means that $\nu \ll 1$ is indeed a small parameter of the problem in the sense that $R[\Phi, F] = O(\nu^2)$. Then the evolution of the function $\Phi(x, t)$ will be described by nearly integrable equation (15) and in this sense will be sufficiently close to the evolution of $\Psi_s(x, t)$ given by (10) at least for period of time defined by $t \ll \nu^{-4}$. We will refer to the respective dynamics as *nonlinear*. If, however, $x\nu \gtrsim 1$ then the first term in (16) becomes exponentially small (since as it follows from (12) decay of $F(x)$ at $x \rightarrow \pm\infty$ is exponentially fast) and the second term is approximately canceled with the nonlinear term in (15). In that case the dynamics is governed by the effectively linear equation.

C. Nonlinear dynamics of a dark soliton.

Suppose that $X(t) = o(\nu^{-1})$. In this case estimates (17) hold for the whole spatial region and one can simplify the expressions for the background with the use of

(18) and (19):

$$F = F_0(x) + O(\nu^4 x^4), \quad F_0(x) \equiv 1 - \frac{\nu^2}{8\rho_0} x^2 \quad (20)$$

and rewrite $R[\Phi, F]$ in the form

$$R[\Phi, F] \approx R[\Phi, F_0] \equiv \frac{\nu^2 x}{2\rho_0} [\Phi_x - x\Phi(|\Phi|^2 - \rho_0)]. \quad (21)$$

Now Eq. (15) can be treated by means of the perturbation theory for dark solitons [16]. In this way, however, one meets a problem: the term proportional to $x\Phi_x$ in the right hand side of (21) belongs to the class of perturbations which effect on the soliton dynamics cannot be described by the adiabatic approximation only. To avoid this difficulty, we make an ansatz

$$\Phi = \phi - i \frac{\nu^2}{2\rho_0} f(t) \frac{\partial \phi}{\partial x}, \quad (22)$$

where

$$f(t) = \int_0^t X(t') dt' + f_0, \quad (23)$$

and the constant f_0 is to be determined later.

Necessity of the renormalization (22) can be justified by full invoking the perturbation theory (see Ref. [16] for details). In order to give here some simple indication on the origin of the phenomenon, we notice that secular terms appearing due to perturbation of a nonlinear equation are eliminated in the so-called adiabatic approximation which is obtained from the exact soliton solution by allowing parameters to be dependent on time. If in our case one substitutes $e^{-i\vartheta/2} \Psi_s(x, t)$, where $\Psi_s(x, t)$ is given by (10), into the left hand side of (3) and computes the imaginary part, one ensures that it is an even function of the spatial coordinate. Thus if $\text{Im} e^{-i\vartheta/2} R[\Phi, F]$ has an odd (with respect to x) component, a secular term originated by such a term cannot be eliminated by any modification of the soliton parameters. This requires introducing additional phase factor $\varphi(x, t)$ [see (27) below]. The peculiarity of such a phase shift, however, is that the imaginary part of the respective term (after multiplying by $\exp(-i\vartheta/2)$) is proportional to $\tanh \eta(x - X(t))$ and thus is zero at $x = X(t)$. Thus if $\text{Im} e^{-i\vartheta/2} R[\Phi, F]$ is not zero at $x = X(t)$, it cannot be eliminated by any modification of the adiabatic theory. The ansatz (22) allows one to count the mentioned ‘‘dangerous’’ term explicitly. Taking into account the explicit form of that term, namely the fact that it is related to translational invariance of the system and is localized about the dark soliton kernel, it can be interpreted as an *internal mode* of a dark soliton excited by spatially varying background.

Now the dynamical equation for ϕ with the accuracy $O(\nu^4)$ reads

$$i\phi_t + \phi_{xx} - 2(|\phi|^2 - \rho_0)\phi = \nu^2 \tilde{R}, \quad (24)$$

where

$$\begin{aligned} \tilde{R} = & \frac{1}{2\rho_0} [(x - X(t))\phi_x - x^2(|\phi|^2 - \rho_0)\phi \\ & + 4if(t)\phi^2\bar{\phi}_x + \frac{\nu^2 f^2(t)}{\rho_0} (2\phi|\phi_x|^2 - \bar{\phi}(\phi_x)^2) \\ & - i\frac{\nu^4 f^3(t)}{2\rho_0^2} \phi_x|\phi_x|^2] \end{aligned} \quad (25)$$

where the terms proportional to the second and third order of $f(t)$ in some cases may be not small (see below).

The perturbation theory can be applied to (24), (25). To this end we pass to new independent variables $(x, t) \rightarrow (\Theta, t)$ where

$$\Theta = \eta(t)(x - X(t)) \quad \text{and} \quad X(t) = Vt + x_0(t) \quad (26)$$

and $\eta(t)$ and $x_0(t)$ are allowed to be dependent on time with the initial conditions $\eta(0) = \eta_0$ and $x_0(0) = X_0$, and look for ϕ in the form

$$\phi(x, t) = e^{i\nu^2 \varphi(x, t)} (\phi_{ad} + \nu^2 \phi_1 + \dots), \quad (27)$$

where

$$\phi_{ad} = \sqrt{\rho_0} e^{i\frac{\vartheta}{2}} \left(\cos \frac{\vartheta}{2} + i \sin \frac{\vartheta}{2} \tanh \frac{\Theta}{2} \right) \quad (28)$$

is the adiabatic approximation. As it has been mentioned above, $\eta(t)$ and $x_0(t)$ are (slow) functions of time, describing variations of the width/depth and velocity of the soliton, respectively. Quantity $X(t)$, which gives a position of the minimum of the soliton intensity must be interpreted as a *coordinate of the soliton center*. By introducing the rapidly varying phase $\varphi(x, t)$ one can satisfy the equation of balance of the momentum [16]

$$P = \frac{1}{2i} \int_{-\infty}^{\infty} (\phi_{\Theta} \bar{\phi} - \phi \bar{\phi}_{\Theta}) d\Theta, \quad (29)$$

which reads

$$\frac{dP}{dt} = - \int_{-\infty}^{\infty} (\tilde{R} \bar{\phi}_{\Theta} + \tilde{R} \phi_{\Theta}) d\Theta \quad (30)$$

(all functions in the integrands are considered to be dependent on the variables (Θ, t)).

In order to find dependence of $\eta(t)$ on time, one can use the conservation law

$$\frac{d\tilde{N}}{dt} = 2 \int_{-\infty}^{\infty} dx \text{Im}(\bar{\phi} \tilde{R}), \quad (31)$$

where

$$\tilde{N} = \int_{-\infty}^{\infty} dx (\rho_0 - |\phi|^2). \quad (32)$$

Direct calculations allow one to ensure that (31), (32) give $d\eta/dt = 0$, and thus the amplitude of the soliton is conserved: $\eta \equiv \eta_0$. This results gives an explanation

of the numerical findings reported in [10, 11, 12]. It is important, however, that it has been obtained in the limit $\eta \gg \nu$ and thus cannot be compared with the outcomes of [13].

Now, computing \tilde{R} and substituting the result in (29) and (30), one obtains subject to the boundary conditions $\lim_{|x| \rightarrow \infty} \varphi(x, t) = 0$:

$$\varphi = -\frac{\nu^2 \eta_0}{4\rho_0} \frac{\Theta}{\cosh^2(\Theta/2)} \int_0^t X(t') dt'. \quad (33)$$

Let us consider a soliton trajectory. After direct substitution of Eq.(25) into Eqs.(A2), (A3) and then substitution of the obtained result into (A1) one can get (see Appendix A)

$$\begin{aligned} \frac{dx_0}{dt} &= -\frac{\nu^2}{3} \left(2 \sin^2 \frac{\vartheta}{2} + 1 \right) \int_0^t X(t') dt' \\ &\quad - \frac{\nu^2 V}{8\rho_0} X^2 - \frac{4\nu^4 V \sin^2 \frac{\vartheta}{2}}{9\rho_0} \left(\int_0^t X(t') dt' \right)^2 \\ &\quad + \frac{2\nu^6 \sin^4 \frac{\vartheta}{2}}{15\rho_0} \left(\int_0^t X(t') dt' \right)^3. \end{aligned} \quad (34)$$

Requiring the initial soliton velocity to be V , i.e. $\frac{dx_0}{dt}|_{t=0} = 0$ one obtains the constant introduced in (23): $f_0 = \frac{(6+\pi^2)}{24} \frac{V}{\rho_0 \eta_0^3} + O(\nu^2 V^2)$.

Below we will argue that the theory is applicable for relatively small velocities, in particular for $V \sim \nu$. This means that we are to restrict the consideration to ϑ close to π . Let us first consider $|\vartheta - \pi| \sim \nu$. This allows one to verify, using Eq. (34), that $X(t)$ in the leading order with respect to ν (designated below as $X_0(t)$) satisfies the equation of the harmonic oscillator

$$\frac{d^2 X_0}{dt^2} + \nu^2 X_0(t) = 0 \quad (35)$$

and thus

$$X_0(t) = \frac{V}{\nu} \sin(\nu t) \quad (36)$$

(where the initial conditions $X_0(0) = 0$, $\dot{X}_0(0) = V$ have been used). Thus, the soliton center, defined as a local minimum of the intensity undergoes oscillatory motion with the frequency which is equal to the frequency of the trap ν . This result also corroborates with previous investigations [10, 12, 13]. Notice that from Eq. (36) and the condition $|X(t)| \lesssim 1$ follows the relation $V \sim \nu$ used above.

Let us now return to expansion (20) and observe that it is still valid if we consider $X \sim \nu^{-1/2}$ (and $\nu^{1/2} \ll 1$). In this case the soliton velocity is allowed to be of order of $\nu^{1/2}$. Then differentiation of (34) with respect to time yields (instead of (35))

$$\frac{d^2 X}{dt^2} + \tilde{\nu}^2 X(t) = \frac{\nu V^3}{\rho_0} \left(\frac{23}{72} \sin(2\nu t) + \frac{1}{10} \sin(3\nu t) \right) \quad (37)$$

where

$$\tilde{\nu}^2 = \nu^2 \left(1 + \frac{2}{9} \frac{V^2}{\rho_0} \right) \quad (38)$$

is the renormalized frequency and in the right hand side $X(t)$ has been substituted by $X_0(t)$ given by (36). Then one computes

$$\begin{aligned} X(t) &= \left(1 + \frac{541}{2160} \frac{V^2}{\rho_0} \right) \frac{V}{\nu} \sin(\tilde{\nu} t) \\ &\quad - \frac{V^3}{\rho_0 \nu} \left(\frac{23}{216} \sin(2\nu t) + \frac{1}{80} \sin(3\nu t) \right). \end{aligned} \quad (39)$$

The obtained result reveals three important features of the dynamics when the soliton velocity increases. First, the frequency of oscillations increases compared with the frequency of the harmonic trap (in the case at hand by $\frac{1}{9} \frac{V^2}{\rho_0}$). Second, the amplitude of oscillations also increases (by the value $\frac{541}{2160} \frac{V^2}{\rho_0}$). Third, there exists a small ($\sim \nu$) frequency mismatch between second harmonic and a double first harmonic and between third harmonics and the triple first harmonic. This leads to slow (compared with the period of soliton oscillations) variation of the amplitude of the periodic motion. Below we will observe all these phenomena in numerical simulations (see Fig. 1).

D. On the Ehrenfest theorem for dark solitons

As was indicated in [10, 12], the frequency of the soliton oscillations can be found with help of the Ehrenfest theorem which must be written for the “center of gravity” of the whole condensate

$$\bar{x}(t) = \frac{1}{N} \int_{-\infty}^{\infty} x |\Psi(x, t)|^2 dx, \quad (40)$$

where

$$N = \int_{-\infty}^{\infty} |\Psi(x, t)|^2 dx \quad (41)$$

is a renormalized number of particles of the whole condensate ($N \sim \mathcal{N}$). Then the coordinate of the dark soliton can be defined as

$$\bar{x}_s(t) = \frac{1}{N_s} \int_{-\infty}^{\infty} x [F(x)]^2 (|\Phi(x, t)|^2 - \rho_0) dx, \quad (42)$$

where

$$N_s = \int_{-\infty}^{\infty} (|\Phi(x, t)|^2 - \rho_0) dx \quad (43)$$

can be interpreted as a *negative mass* of a dark soliton.

One can easily show that $\bar{x}_s(t)$ coincides with $X_0(t)$, defined in subsection II C, only in the leading order and at initial stages of evolution, and thus cannot be treated as a coordinate of the soliton center in a general case.

Indeed, it is straightforward to show that $\bar{x}_s(t)$ obeys the exact “Newton law”

$$\frac{d^2\bar{x}_s}{dt^2} = - \int_{-\infty}^{\infty} \frac{\partial V_{trap}}{\partial x} |\Psi(x,t)|^2 dx, \quad (44)$$

which in the case at hand is reduced to the equation for the harmonic oscillator. Then, taking into account the initial condition in the form

$$\Psi(x, 0) = F(x) \cdot \Phi_s(x, 0), \quad (45)$$

which corresponds to the form of the solution given by (11), one computes

$$\bar{x}_s(t) = \frac{V}{\nu} \sin(\nu t), \quad (46)$$

which is an exact formula (notice that Eq. (36) is approximate).

Thus, we have obtained that in the lowest order of ν a dark soliton with a small velocity $V \sim \nu$ undergoes oscillatory behavior which emerges both from the perturbation theory for solitons and from the Ehrenfest theorem. Such a behavior is confirmed by the direct numerical simulations (see Fig.1c below, where $\nu = 0.2$, and $V \approx 0.14$). However, significant deviations from the Ehrenfest theorem are observed with growth of the initial dark soliton velocity [c.f. (46) and (39)].

E. Numerical simulations of the one-soliton dynamics.

To verify the above findings, we have done extensive numerical simulations of the dark soliton dynamics which is governed by the evolution equation Eq. (3) subject to the initial conditions (45). In Fig. 1 we present a dark soliton trajectories $X(t)$, which numerically were defined as the coordinate of the local minimum of the soliton, from the long-time simulations. Although, strictly speaking, only the case depicted in Fig. 1c corresponds to the perturbation theory developed above, all the plots display several features qualitatively coinciding with the theoretical predictions.

First, the choice of the form of the background as an eigenfunction of the problem (12) indeed allows one to follow the dynamics up to hundreds of periods of oscillations, if initially soliton had large enough amplitude, i.e. one still can identify an entity called dark soliton.

Second, the dynamics of such defined $X(t)$ displays relatively large deviations from that, which would follow from the Ehrenfest theorem, when \bar{x}_s is identified with the soliton coordinate. Namely, in all the cases the frequency of the soliton oscillations is higher than the frequency, predicted from the Ehrenfest theorem (see (46)). The observed frequency change is of order of a few percents ($\sim 3\%$ in Fig. 1b) which agrees with prediction (38).

Third, one observes that the amplitude of oscillations are larger than V/ν predicted by Ehrenfest theorem and displays the periodic modulation. All these differences increase with growth of the initial soliton velocity V . This behavior is also in qualitative agreement with the result (39) obtained within the framework of the perturbation theory.

FIG. 1: Dark soliton trajectories $X(t)$ (solid lines): for $\rho_0 = 1$ and different initial parameters (a) $\vartheta_0 = 2$; (b) $\vartheta_0 = 2.5$; (c) $\vartheta_0 = 3$, and the trajectories following from the Ehrenfest theorem \bar{x}_s (dashed lines); Figure (d) shows soliton trajectories for $\vartheta_0 = 2$ and different amplitudes $\rho_0 = 0.5; 1; 2$ (solid, dotted and dashed line correspondingly). The parameter of harmonic trap potential is $\nu = 0.2$.

It is to be emphasized that all above effects become easily visible after several periods of oscillations, while during the first period they closely follow the “Ehrenfest trajectory” given by (46) or (36). This coincidence of the trajectories has been observed in Refs. [10, 11, 12, 13] where only few cycles were counted. Our numerical simulations of first turning point also have shown that if an initial soliton is deep enough (what corresponds to small values of V), then the amplitude $a_{theor} = V/\nu$ found from Eq. (36) and amplitude a_{num} calculated numerically as a local minimum of the intensity practically coincide with each other, which is illustrated by Table I.

TABLE I: Amplitudes of oscillations calculated theoretically $a_{theor} = V/\nu$ and from the direct simulation of Eq. (3) a_{num} for $\rho_0 = 1$ and different initial values of the parameter ϑ_0 and for two different trap potentials.

| ϑ_0 | $\nu = 0.2$ | | $\nu = 0.1$ | |
|---------------|-------------|-----------|-------------|-----------|
| | a_{theor} | a_{num} | a_{theor} | a_{num} |
| 1 | 8.78 | 9.17 | 17.55 | 17.99 |
| 1.25 | 8.11 | 8.33 | 16.22 | 16.59 |
| 1.5 | 7.32 | 7.49 | 14.63 | 14.96 |
| 1.75 | 6.41 | 6.56 | 12.82 | 13.09 |
| 2 | 5.40 | 5.54 | 10.80 | 11.01 |
| 2.25 | 4.31 | 4.42 | 8.62 | 8.77 |
| 2.5 | 3.15 | 3.23 | 6.31 | 6.41 |
| 2.75 | 1.95 | 1.99 | 3.89 | 3.95 |
| 3 | 0.71 | 0.73 | 1.42 | 1.44 |

In Fig. 2 we present snapshots of the dark soliton evolution for a region of parameters when the perturbation theory strictly speaking is not applicable ($\vartheta_0 = 2$ and $\rho_0 = 1$ correspond to $V \approx 1.08$ and thus $V > \nu$). One can observe rather strong non-adiabatic effects which manifest themselves in a significant deformation of a soliton shape, namely in formation of leading and trailing waves before and behind the soliton in the “background” distribution.

FIG. 2: The reduced shape of the initial distribution computed as $|F(x)|^2 - |\Psi(x, t)|^2$ (solid line) for $\vartheta_0 = 2$ and $\nu = 0.2$ at (a) $t = 0$; (b) $t = 3$; (c) $t = 7.3$; (d) $t = 11$; (e) $t = 15.2$; (f) $t = 18$. Thin dashed lines show the background $|F(x)|^2$.

Some features of the dark soliton dynamics can be understood much better if one investigates in detail the turning points. First of all, taking into account that only a black soliton has zero velocity, it is natural to suppose that at the turning points the soliton becomes black. The less is the soliton depth, the farther from the center is a turning point, and hence the greater is the amplitude of the oscillations. This correlation between variations of the depth and of the amplitude becomes evident if one compares the results depicted in Fig. 3 and in Fig. 1. As it has been mentioned in the previous section, these oscillations are due to mismatch between the first and higher harmonics. In all numerical studies carried out we have observed oscillations similar to ones shown in Fig. 1. They can be explained by the mismatch $3(\nu - \tilde{\nu})$. We however did not observe pronounced oscillations due to difference in the second harmonics, i.e. due to $2(\nu - \tilde{\nu})$. We attribute this behavior to the fact that non-adiabatic effects due to the third harmonics are effectively much stronger than due to the second one.

FIG. 3: Time dependence of the depth of the dark soliton for $\rho_0 = 1$, $\nu = 0.2$ and different initial parameters $\vartheta_0 = 2; 2.5; 3$ (curves 1,2,3 correspondingly).

FIG. 4: Behavior of the hydrodynamic velocity $v = \partial\varphi_{tot}/\partial x$ in the vicinity of a turning point for initial parameters $\vartheta_0 = 2$ and $\nu = 0.3$. Δt is a time counted from the turning point. Left column is an output of direct numerical simulations and right one is formally obtained from the perturbation theory (see the text).

Finally, an important effect accompanying changes of the soliton velocity is a change of the total phase, $\varphi_{tot} = \arg \Phi(x, t)$, of the solution which is especially significant at the turning points. Our numerical studies of the phase evolution are shown in Fig. 4, where in the left column we depicted the hydrodynamical velocity v defined as $v = \partial\varphi_{tot}/\partial x$ (see also the next section). As one can see, near the turning point hydrodynamic velocity changes dramatically making a flip (see Figs. 4b,c), and after that soliton moves in the opposite direction (Fig. 4d). In the right column we show the phase variation during the reflection formally computed using for-

mulas of the perturbation theory, i.e. Eqs. (10), (22), (27), and (28). Comparing the two sets of graphics one observes remarkable similarity of the main features (and, what is more important, the main scales) of the dynamics in the both cases. Three differences, however, are observable. First, the phase of the direct numerical solution displays asymmetry, which is naturally explained by the asymmetric non-adiabatic modulation of the soliton shape (c.f. Fig. 2). Second, spatial locations of the turning points are slightly different. Third, asymptotic values of the hydrodynamical velocity far from the soliton center differ as well. These discrepancies are explained by the fact that the case under consideration does not satisfy the conditions of the applicability of the adiabatic approximation, and thus one can expect that the last one can give only right orders of magnitude of the parameters and indicate correctly the main qualitative features (what is indeed observed in comparison of the two sets of graphics).

III. FORMATION OF SOLITONS FROM LARGE INITIAL EXCITATION

The problem of evaluation of parameters of dark solitons formed from a large initial excitation on a constant background is formally solved by the inverse scattering method [9]. In the framework of this method, the NLS equation is associated with the so-called Zakharov-Shabat linear spectral problem [9], and soliton parameters are related with the eigenvalues of this problem calculated for a given initial condensate wave function $\Psi(x, 0)$. If the initial disturbance is large enough, so that the linear spectral problem possesses many eigenvalues, then a well-known quasi-classical method can be applied for their calculation. As was shown in recent paper [17], a generalized Bohr-Sommerfeld quantization rule is very convenient for this aim.

To formulate this rule, it is convenient to introduce a new small parameter ε , $\varepsilon \ll 1$, into Eq. (3) by means of replacements $x = x'/\varepsilon$, $t = t'/\varepsilon$, $\nu = \nu'\varepsilon$, so that the equation transforms to

$$i\varepsilon \frac{\partial \Psi}{\partial t} + \varepsilon^2 \frac{\partial^2 \Psi}{\partial x^2} - 2|\Psi|^2 \Psi = \frac{1}{2} \nu'^2 x^2 \Psi, \quad (47)$$

where we have omitted for simplicity the primes in the new variables. Then the limit $\varepsilon \ll 1$ corresponds to formation of a large number of solitons from an initial disturbance with parameters of order of magnitude $O(1)$ (see [17]). In framework of the inverse scattering transform method the NLS equation, i.e. Eq. (47) with the zero right hand side, is treated as a compatibility condition of two linear equations for auxiliary function χ , which we write down in the form

$$\varepsilon^2 \chi_{xx} = \mathcal{A}\chi, \quad \chi_t = -\frac{1}{2} \mathcal{B}\chi_x + \mathcal{B}_x \chi, \quad (48)$$

(equivalent to the Zakharov-Shabat problem; see [18,

19)], where

$$\mathcal{A} = -\left(\lambda - \frac{i\varepsilon\Psi_x}{2\Psi}\right)^2 + |\Psi|^2 - \varepsilon^2\left(\frac{\Psi_x}{2\Psi}\right)_x, \quad (49)$$

$$\mathcal{B} = 2\lambda + \frac{i\varepsilon\Psi_x}{\Psi}. \quad (50)$$

The first equation (48) may be considered as a second order scalar spectral problem with a given “potential” Ψ and λ playing the role of the spectral parameter. When $\Psi(x, t)$ evolves according to Eq. (47) with $\nu = 0$, the eigenvalues λ_n of this problem do not change with time t , and each eigenvalue corresponds to a soliton created from the initial pulse. To investigate the limit $\varepsilon \ll 1$, let us represent the condensate wave function in the form

$$\Psi(x, t) = \sqrt{\rho(x, t)} \exp\left(\frac{i}{\varepsilon} \int^x v(x', t) dx'\right), \quad (51)$$

where $\rho(x, t)$ has a meaning of the condensate density and $v(x, t)$ is the hydrodynamic velocity. Indeed, substitution of (51) into (47) yields the system

$$\begin{aligned} \frac{1}{2}\rho_t + (\rho v)_x &= 0, \\ \frac{1}{2}v_t + vv_x + \rho_x + \varepsilon^2\left((\rho_x^2 - 2\rho\rho_{xx})/8\rho^2\right)_x &= -\frac{1}{2}\nu^2x, \end{aligned} \quad (52)$$

which for $\varepsilon \rightarrow 0$ takes the form of hydrodynamic equations. For smooth enough functions $\rho(x, t)$ and $v(x, t)$, when

$$|\varepsilon\rho_x/\rho| \ll \rho, \quad \text{and} \quad |\varepsilon v_x| \ll \rho, \quad (53)$$

what corresponds to neglecting the space derivatives in \mathcal{A} , spectral problem (48) transforms into

$$\varepsilon^2\chi_{xx} = \left[-(\lambda + v/2)^2 + \rho\right]\chi. \quad (54)$$

It is to be mentioned here that conditions (53) are nothing but the conditions of applicability of the well-known hydrodynamical approach when due to a relatively high density the two-body interactions are strong enough and one can neglect the “quantum pressure” (see, e.g. [4]).

FIG. 5: Schematic plot of the Riemann invariant λ^+ given by Eq.(55) (thick solid line); thin solid line shows the Riemann invariant for disturbance with respect to uniform background; dashed line shows background without disturbance. x^* denotes the position of localized disturbance and $\Delta F(x^*) = 1 - F(x^*)$ is the change of the condensate density because of condensate non-uniformity. d is characteristic scale of the initial disturbance. The horizontal lines of different width indicate positions of eigenvalues λ_n and the width of each line characterizes the lifetime of the corresponding solitons (the thicker is a line, the smaller is the lifetime).

Equation (54) has a formal analogy with a stationary Schrödinger equation for a quantum-mechanical motion of a particle in the “energy-dependent” potential, i.e. the

potential depending on the spectral parameter λ . According to the mentioned above independence of the eigenvalues λ_n on time, they can be calculated with the use of the initial distributions $\rho(x, 0)$ and $v(x, 0)$. Since we are interested in such initial data which give rise to creation of large number of solitons, this means that functions $\rho(x, 0)$ and $v(x, 0)$ correspond to the problem (54) with a large number of eigenvalues. Then the quasi-classical approach can be used for their calculation [17]. To clarify this method, we have shown schematically in Fig. 5 a plot of the “Riemann invariant”

$$\lambda^+ = -v(x, 0)/2 + \sqrt{\rho(x, 0)} \quad (55)$$

which plays a role of the “quantum-mechanical potential” for the problem (54). (The second Riemann invariant $\lambda^- = -v(x, 0)/2 - \sqrt{\rho(x, 0)}$ can be considered in the same way.) The Riemann invariant for the same disturbance but with respect to uniform background $F(x) = 1$ is shown for comparison by thin solid line. We see that in both cases there is a “potential well”, but for the nonuniform background case the eigenvalues acquire imaginary part (“decay width”) due to tunnelling effect. This means that dark solitons in confined condensate have a finite life-time τ_n determined by the imaginary part of the eigenvalue λ_n , what correlates with the above mentioned fact that in this case the soliton is not a “well-defined” object. Nevertheless, it makes sense to speak about solitons in a confined condensate, if their life-times τ_n are much greater than the period $\simeq 2\pi/\nu$ of their oscillations discussed in the preceding Section. It is clear that “shallow” solitons with small τ_n do not survive in the confined condensate, so that λ_n with values close to the top of the “potential barrier” do not correspond to any real solitons. On the contrary, in the case of the uniform background discussed in [17] all eigenvalues correspond to real solitons appearing eventually from the initial pulse. In multi-soliton problem there is also one more scale of time equal to time of formation of solitons from the initial pulse. For deep enough solitons it can be estimated by the order of magnitude as time necessary for solitons with velocity $|V_n| = 2|\lambda_n|$ (see below) to pass the distance equal to the width d of the initial problem. For the problems under consideration, this time $\sim d/2|\lambda_n|$ must be much less than the period $2\pi/\nu$. Thus, we are interested in the eigenvalues λ_n which satisfy inequalities

$$\tau_n \gg \frac{2\pi}{\nu} \gg \frac{d}{2|\lambda_n|}. \quad (56)$$

It is clear that there are no these reservations in the case of uniform background [17] where formally $\tau_n = \infty$ and one can wait long enough to observe formation of soliton with any value of λ_n .

To calculate the real parts of the eigenvalues λ_n corresponding to deep solitons, one can use the generalized

Bohr-Sommerfeld quantization rule

$$\frac{1}{\varepsilon} \int_{x_n^-}^{x_n^+} \sqrt{\left(\lambda_n + \frac{1}{2}v(x,0)\right)^2 - \rho(x,0)} dx = \pi \left(n + \frac{1}{2}\right),$$

$$n = 0, 1, 2, \dots, M, \quad (57)$$

with given initial distributions $\rho(x,0)$ and $v(x,0)$. We suppose here that the integrand has only one maximum and x_n^+ and x_n^- are the points where the integrand function vanishes: they depend on λ_n and are chosen so that the relationship (57) is satisfied (see Fig. 5). Analytical form of each emerging soliton in an asymptotic region where it is well separated from other solitons (i.e. in the limit $t \rightarrow \infty$) is expressed in terms of λ_n as follows:

$$\rho_s^{(n)}(x,t) = \rho_0 - \frac{\rho_0 - \lambda_n^2}{\cosh^2 \left[\sqrt{\rho_0 - \lambda_n^2} (x - 2\lambda_n t) / \varepsilon \right]}, \quad (58)$$

$$v_s^{(n)}(x,t) = \lambda_n \left(\rho_0 / \rho_s^{(n)} - 1 \right). \quad (59)$$

As it is clear, formulas (58), (59) and (10) with $\vartheta = \vartheta_n$, $\eta_0 = \eta_n$, and $V = V_n$, where the parameters are connected by the relation $\lambda_n = \sqrt{\rho_0} \cos(\vartheta_n/2)$, represent the same one-soliton solution. Thus, the last formula allows one to find initial values of ϑ_n for solitons emerging from the dark excitation of the condensate with given initial distributions of $\rho(x,0)$ and $v(x,0)$ against a constant uniform background.

If the background is not uniform but changes in space in the intervals of integration in (57), then we can apply the same method with ρ_0 replaced by the value of the background density $F^2(x^*)$ at the place x^* of the localized initial excitation (see Fig. 5).

We have used this approach for finding soliton parameters for different types of initial excitations: (i) excitations of the density $\rho(x)$ [1], (ii) excitation of the hydrodynamic velocity $v(x)$ (“phase imprinting method”) [2, 15] and (iii) collision of condensates [11].

(i) In the first case of the density disturbance the initial data were taken in the form

$$\rho(x,0) = \left(1 - \frac{\alpha}{\cosh(x)}\right)^2, \quad v(x,0) = 0, \quad (60)$$

where the parameter α measures the strength of the disturbance. We have chosen the following values of the parameters: $\alpha = 0.8$, $\nu = 0.2$, $\varepsilon = 0.3$. The values of λ_n for the three deepest solitons calculated with the use the Bohr-Sommerfeld rule (57) are shown in Table II together with the corresponding values of ϑ_n and amplitudes $a_{theor}^{(n)}$ calculated for these soliton from (36) and found from numerical solution of (3) with the initial data (60). The discrepancy is less than 10% and is caused, apparently, by the fact that in our case the created solitons did not reach yet the asymptotic values of their velocities $V_n = 2\lambda_n$. Besides that, numerical calculations show

TABLE II: Parameters of solitons created from initial intensity disturbance

| n | $\lambda^{(n)}$ | $\vartheta^{(n)}$ | $a_{theor}^{(n)}$ | $a_{num}^{(n)}$ |
|-----|-----------------|-------------------|-------------------|-----------------|
| 0 | 0.41 | 2.29 | 2.74 | 2.48 |
| 1 | 0.65 | 1.72 | 4.35 | 4.23 |
| 2 | 0.80 | 1.28 | 5.42 | 5.54 |

that the “initial coordinates” of solitons created from the initial pulse cannot be identified exactly with $X(0) = 0$. This is the reason why solitons created from one initial pulse do not reverse simultaneously their directions of motion even during the first period of oscillations in the confined condensate. This phenomenon is illustrated in Fig. 6, where the density $\rho(x,t)$ and hydrodynamic velocity $v(x,t)$ of the condensate are shown as functions of x at the moments when two solitons in each train have already reversed the direction of their propagation and are moving to the center, while the other two solitons are still moving from the center. This process of “solitons reflection from the potential well” takes about 20% of the whole period $2\pi/\nu$ of their oscillations.

FIG. 6: Space distribution of the density of a BEC (a) and of its hydrodynamic velocity (b) in the harmonic trapped potential with $\nu = 0.3$ at time $t = 4.24$ with initial excitation taken in the form of pulse (60) with $\rho_0 = 1$, $\alpha = 0.8$ and $\varepsilon = 0.3$.

FIG. 7: Space distribution of density of BEC (a) and its hydrodynamic velocity (b) in the harmonic trapped potential with $\nu = 0.3$ at time $t = 1$ without (dotted line) and with (solid line) initial excitation that is taken as a phase step with $\rho_0 = 1$, $\alpha = 4$, $\kappa = 0.4$ and $\varepsilon = 1$.

(ii) For illustration of the process of solitons formation by the phase imprinting method we have chosen the initial conditions in the form

$$\rho(x,0) = F^2(x), \quad v(x,0) = \frac{\alpha}{\cosh^2(\kappa x)}. \quad (61)$$

Again the solitons parameters can be calculated with the use of the Bohr-Sommerfeld quantization rule (57) and their values correspond well to numerical simulation. In particular, the Bohr-Sommerfeld rule gives correct number of solitons and signs of their initial velocities. As one can see in Fig. 7, at first the deepest soliton moves to the right but the hydrodynamic velocity distribution corresponds to its motion to the left. Only when the local density minimum touches the x axis, the velocity distribution makes a flip and after that it corresponds to the predicted direction of the soliton propagation (see Fig. 8). All solitons predicted by the Bohr-Sommerfeld quantization rule can be observed during some time interval after their formation (see Figs. 8,9). However, in

FIG. 8: The same as on Fig. 7 at $t = 1.5$.FIG. 9: The same as on Fig. 7 at $t = 4$.

the case of initial data (61) we observe also strong non-soliton contribution into excitation of the condensate (see Fig. 7) which leads to much more complicated picture of its evolution. One may say that in this case solitons move along background varying with time and the influence of this time dependence is not small on the contrary to the previous case of the density disturbance. As a result, the motion of solitons cannot be described as (almost) harmonic oscillations along constant nonuniform background. But even in this case quasi-classical method of finding the solitons parameters yields quite accurate description of solitons motion for times less than $2\pi/\nu$.

(iii) Formation of dark solitons can be observed also during collision of two separated condensates which move under influence of the trap potential [11]. Taking the initial conditions in the form

$$\begin{aligned} \rho(x, 0) &= \exp[-\kappa(x - \xi)^2] + \exp[-\kappa(x + \xi)^2], \\ v(x, 0) &= 0 \end{aligned} \quad (62)$$

we have solved Eq. (3) numerically. It was found that these two condensates oscillate in the trap potential and interact with each other in quite complicated way when they overlap with each other. Since the initial data (62) lead to a number of eigenvalues $\lambda^{(n)}$, one may expect that during the collision of two condensates the corresponding number of dark solitons must be observed. This is indeed the case as one can see in Fig. 10, where the density and the hydrodynamic velocity distributions are shown at the moment of maximal overlap of two condensates whose initial density distributions are indicated by dotted lines. The number of solitons matches very well with that predicted by the Bohr-Sommerfeld quantization rule, but their motion cannot be presented as propagation with slowly changing parameters along constant nonuniform background.

FIG. 10: Formation of dark solitons (solid line) during the collision of two initially separated condensates (dotted line) corresponding to the initial data (62) with parameters $\kappa = 0.5$, $\xi = 8$ and $\varepsilon = 0.5$ in harmonic trap potential $\nu = 0.2$ at $t = 4$. a) density of BEC; b) hydrodynamic velocity.

Thus, quasi-classical approach provides simple and effective method of calculation of the parameters of solitons arising from large enough initial disturbance. This method can be used for estimation of these parameters in the today experiments with BEC solitons.

IV. DISCUSSION AND CONCLUSION

In the present paper we have investigated the evolution of localized excitations in a quasi-1D BEC with a positive scattering length confined by a harmonic trap potential. It has been shown that in the case of a single dark soliton the evolution can be considered as a newtonian one only at very low velocities and, hence, big depths of the soliton and at a large enough effective longitudinal size of the condensate. Then the dynamics becomes near-integrable and the perturbation theory for dark solitons can be used. Non-adiabatic effects become essential when one considers long-time dynamics, i.e. dynamics when soliton makes several oscillations. These effects are: increase of the frequency of soliton oscillations; increase of the amplitude of oscillations, which, besides that, changes periodically with a frequency much less than the frequency of the oscillations themselves; change of a soliton shape during the evolution.

Main effects observed in non-newtonian dynamics of a soliton are described qualitatively by the perturbation theory for dark solitons. In particular, the theory allows one to justify the choice of the shape of the background which supports many-cycle dynamics of a soliton without substantial change of its shape. The present study, however, leaves open a question about non-adiabatic deformation of a soliton shape. This requires careful study of the first order perturbation theory which can be made, say, with the use the Green function approach (see [16]) for the respective linearized problem.

The existence of an inhomogeneous background becomes especially important when initially multi-soliton pulses are under consideration. Then, compared to the integrable case with constant background, new temporal scales appear in the problem. They are associated with the harmonic oscillator frequency and finite lifetime of solitons. The life-time decreases with the soliton amplitude, which leads to rather rapid disappearance of shallow dark solitons. Generally speaking, a soliton with a small amplitude can even lose its meaning at all when it is considered against a nonuniform background. Indeed, returning to the condition of smallness of the soliton width $\sim 1/\eta$ compared with the linear oscillator length $\sim 1/\nu$, one must require $\eta \gg \nu$ for a soliton to be meaningful. Recalling now that $a_{theor} \leq \sqrt{\rho_0}/\nu$ where a_{theor} is an amplitude of soliton oscillations, what follows from the Ehrenfest theorem, one concludes that it makes sense to speak about the oscillations of a soliton in the case when $a_{theor} < 1/\nu$, i. e. when $\rho_0 \sim 1$. If ρ_0 is large enough, then the small amplitude soliton can reach a region of an exponentially decaying tail of the condensate distribution already during the first half-a-period of oscillations. In that region the dynamics is essentially linear and thus the pulse will disappear due to dispersion effects as it happens with linear wave-packets. In order to estimate amplitudes of the background at which such behavior is observable, we take into account that the effective nonlinearity, determined from (15), can be esti-

mated as $\rho_0 \exp(-\nu^2 a_{theor}^2)$ and thus it become of order of 10^{-2} already at $\rho_0 \approx 6.5$.

In the context of the above findings a natural question arises about detecting soliton parameters. In connection with this question it is relevant to mention that motion of the soliton is accompanied with the hydrodynamic flow with velocity $v(x, t)$ and the corresponding matter current, which density in the dimensionless units is $J(x, t) = \rho(x, t)v(x, t)$. Dependence of these two quantities on time is periodic. Their dependence on the spatial coordinate is also non-monotonic. Thus, by detection of the velocity and current distribution allows one to make an estimate of the dark soliton parameters.

Acknowledgements

A.M.K. is grateful to the staff of Centro de Física da Matéria Condensada, Universidade de Lisboa, for kind hospitality. The work of V.A.B. has been supported by the FCT fellowship SFRH/BPD/5632/2001. The work of A.M.K. in Lisbon has been supported by the Senior NATO Fellowship. A.M.K. thanks also RFBR (Grant 01-01-00696) for partial support. V.V.K. acknowledges support from the Programme “Human Potential-Research Training Networks”, contract No. HPRN-CT-2000-00158.

APPENDIX A

For the sake of completeness here we reproduce the dynamical equation for $x_0(t)$ which is derived in [16] (notice that the sign between the second term in the right hand side, is corrected):

$$\begin{aligned} \frac{dx_0}{dt} = & \int_{-\infty}^{\infty} d\Theta \left\{ \frac{1}{\eta_0 \eta} \widehat{R}'_+(\Theta, t) \right. \\ & + \frac{V}{\eta_0^2 \eta} \left(\frac{\Theta/2}{\cosh^2(\frac{\Theta}{2})} + \tanh \frac{\Theta}{2} \right) \widehat{R}''_-(\Theta, t) \\ & - \frac{4\rho_0 \eta}{\eta_0^3} \int_0^t dt' \frac{\widehat{R}''_+(\Theta, t')}{\sinh \Theta} \left[\left(1 - \frac{V^2}{\rho_0} \right) \tanh \frac{\Theta}{2} \right. \\ & \left. \left. + \frac{V^2}{4\rho_0} \Theta \left(1 - \frac{3}{2} \frac{1}{\cosh^2(\frac{\Theta}{2})} \right) \right] \right\} \quad (A1) \end{aligned}$$

where notations

$$\widehat{R}'_{\pm}(\Theta, t) = \frac{1}{2} \text{Re} \left[\varepsilon \widetilde{R}(\Theta, t) \pm \varepsilon \widetilde{R}(-\Theta, t) \right], \quad (A2)$$

$$\widehat{R}''_{\pm}(\Theta, t) = \frac{1}{2} \text{Im} \left[\varepsilon \widetilde{R}(\Theta, t) \mp \varepsilon \widetilde{R}(-\Theta, t) \right]. \quad (A3)$$

Here \widetilde{R} is determined by Eq.(25).

-
- [1] M. R. Andrews, D. M. Kurn, H.-J. Miesner, D. S. Durfee, C. G. Townsend, S. Inouye, and W. Ketterle, Phys. Rev. Lett. **79**, 553 (1997).
- [2] S. Burger, K. Bongs, S. Dettmer, W. Ertmer, K. Sengstock, A. Sanpera, G.V. Shlyapnikov, and M. Lewenstein, Phys. Rev. Lett. **83**, 5198 (1999).
- [3] J. Denschlag, J.E. Simsarian, D.L. Feder, C.W. Clark, L.A. Collins, J. Cubizolles, L. Deng, E.W. Hagley, K. Helmerson, W.P. Reinhardt, S.L. Rolston, B.I. Schneider, and W.D. Phillips, Science **287**, 97 (2000).
- [4] F. Dalfovo, S. Giorgini, L.P. Pitaevskii, and S. Stringary, Rev. Mod. Phys. **71**, 463 (1999).
- [5] K. Berg-Sorensen and K. Molmer, Phys. Rev. A **58**, 1480 (1998).
- [6] V.V. Konotop and M. Salerno, Phys. Rev. A **65**, 021602 (2002).
- [7] W. Zhang, D.F. Walls, and B.C. Sanders, Phys. Rev. Lett. **72**, 60 (1994); P.O. Fedichev, A.E. Muryshev, and G.V. Shlyapnikov, Phys. Rev. A **60**, 3220 (1999).
- [8] K.E. Strecker, G.B. Partridge, A.G. Truscott, and R.G. Hulet, Nature **417**, 150 (2002).
- [9] V.E. Zakharov and A.B. Shabat, Sov. Phys. JETP **34**, 62 (1972).
- [10] W.P. Reinhardt and C.W. Clark, J. Phys. B **30**, L785 (1997).
- [11] T.F. Scott, R.J. Ballagh, and K. Burnett, J. Phys. B **31**, L329 (1998).
- [12] Th. Busch and J.R. Anglin, Phys. Rev. Lett. **84**, 2298 (2000).
- [13] G. Huang, M.G. Velarde, and V.A. Makarov, Phys. Rev. A **64**, 013617 (2001).
- [14] R. Dum, J.I. Cirac, M. Lewenstein, and P. Zoller, Phys. Rev. Lett. **80**, 2972 (1998).
- [15] Biao Wu, Jie Liu, and Qian Niu, Phys. Rev. Lett. **88**, 034101 (2002).
- [16] V. V. Konotop and V. E. Vekslerchik, Phys. Rev. E **49**, 2397 (1994).
- [17] A.M. Kamchatnov, R.A. Kraenkel, and B.A. Umarov, Phys. Rev. E **66**, 036609 (2002).
- [18] S.J. Alber, Complex deformations of integrable Hamiltonians over generalized Jacobi varieties, in *Nonlinear Processes in Physics*, Eds. A.S. Fokas, D.J. Kaup, A.C. Newell, and V.E. Zakharov, (Berlin: Springer) p. 6, 1993.
- [19] A.M. Kamchatnov and R.A. Kraenkel, J. Phys. A **35**, L13 (2002).
- [20] D.L. Feder, M.S. Pindzola, L.A. Collins, B.I. Schneider, and C.W. Clark, Phys. Rev. A **62**, 053606 (2000).

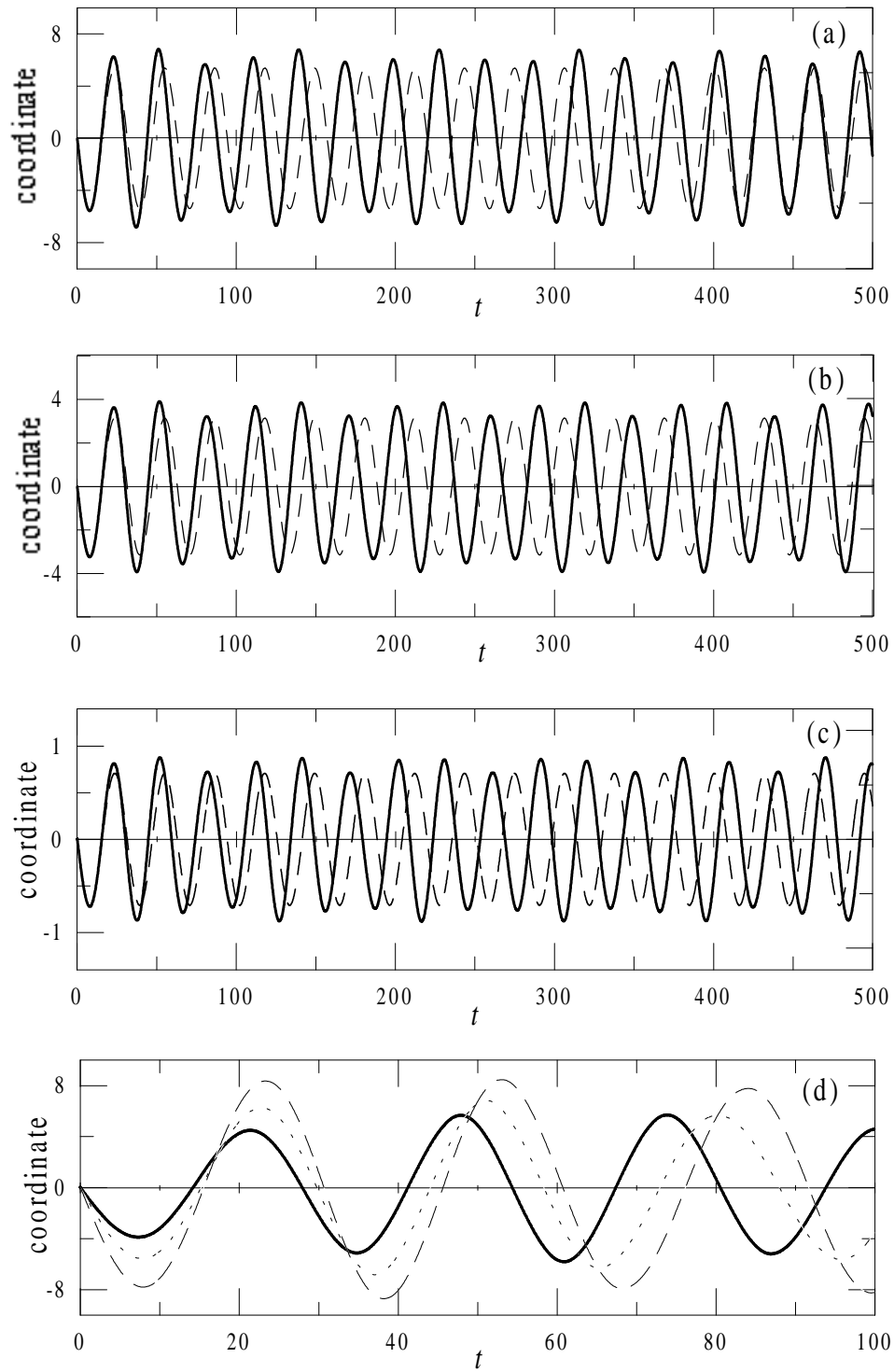


Fig.1

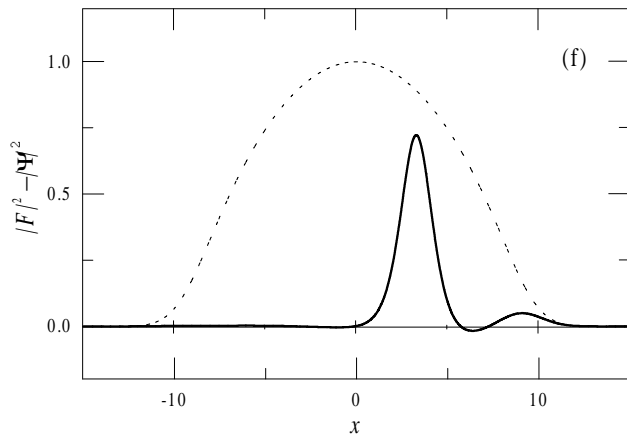
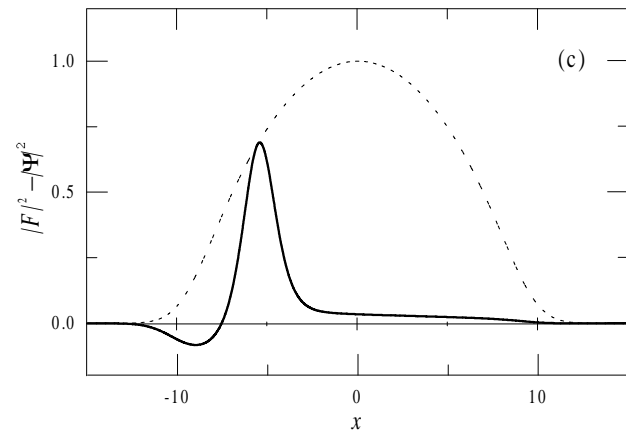
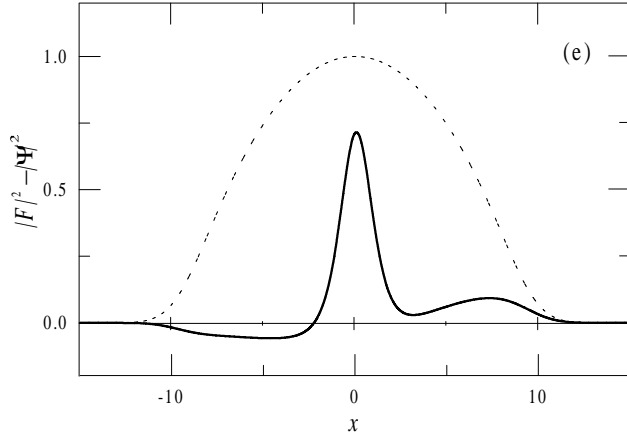
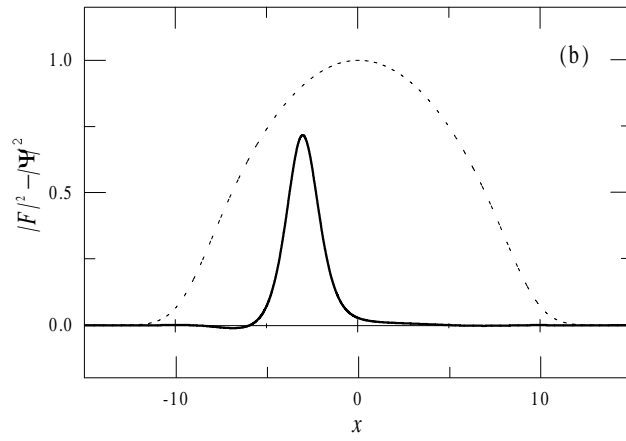
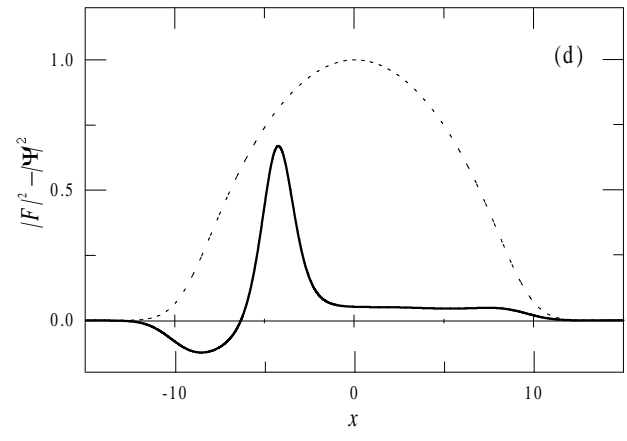
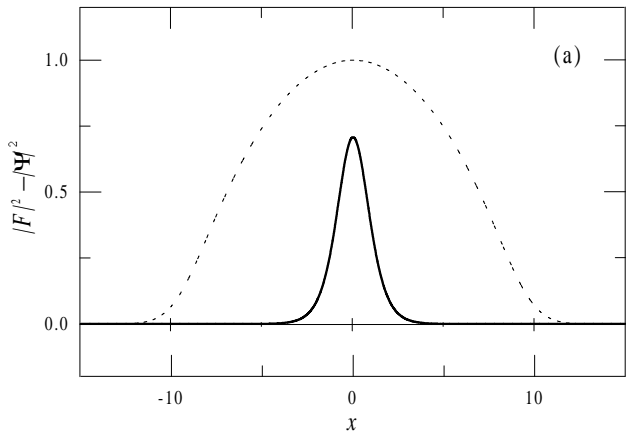


Fig.2

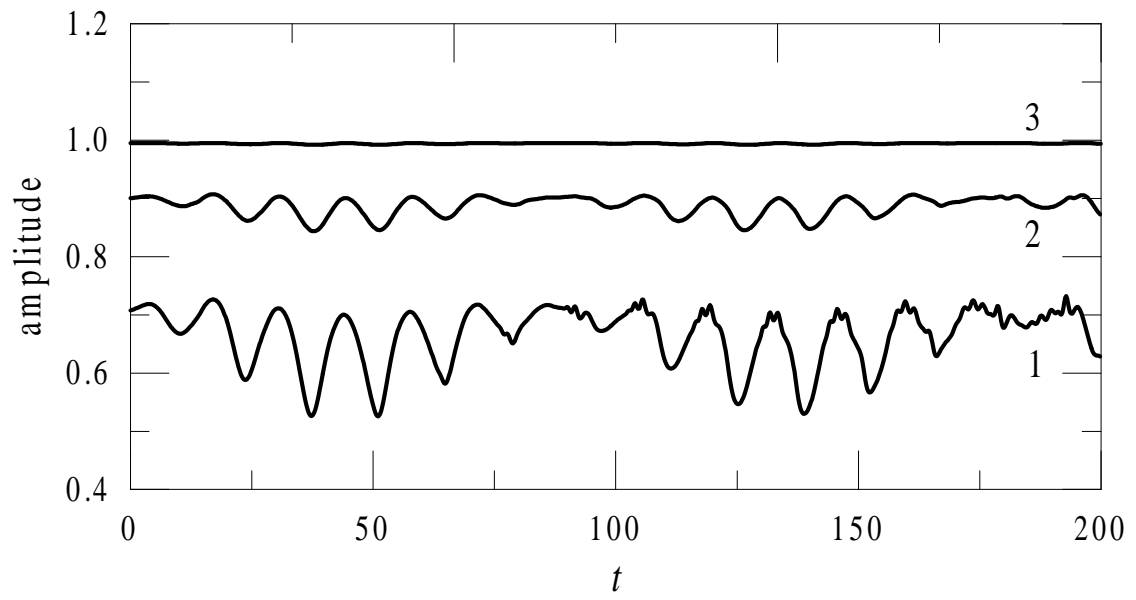


Fig.3

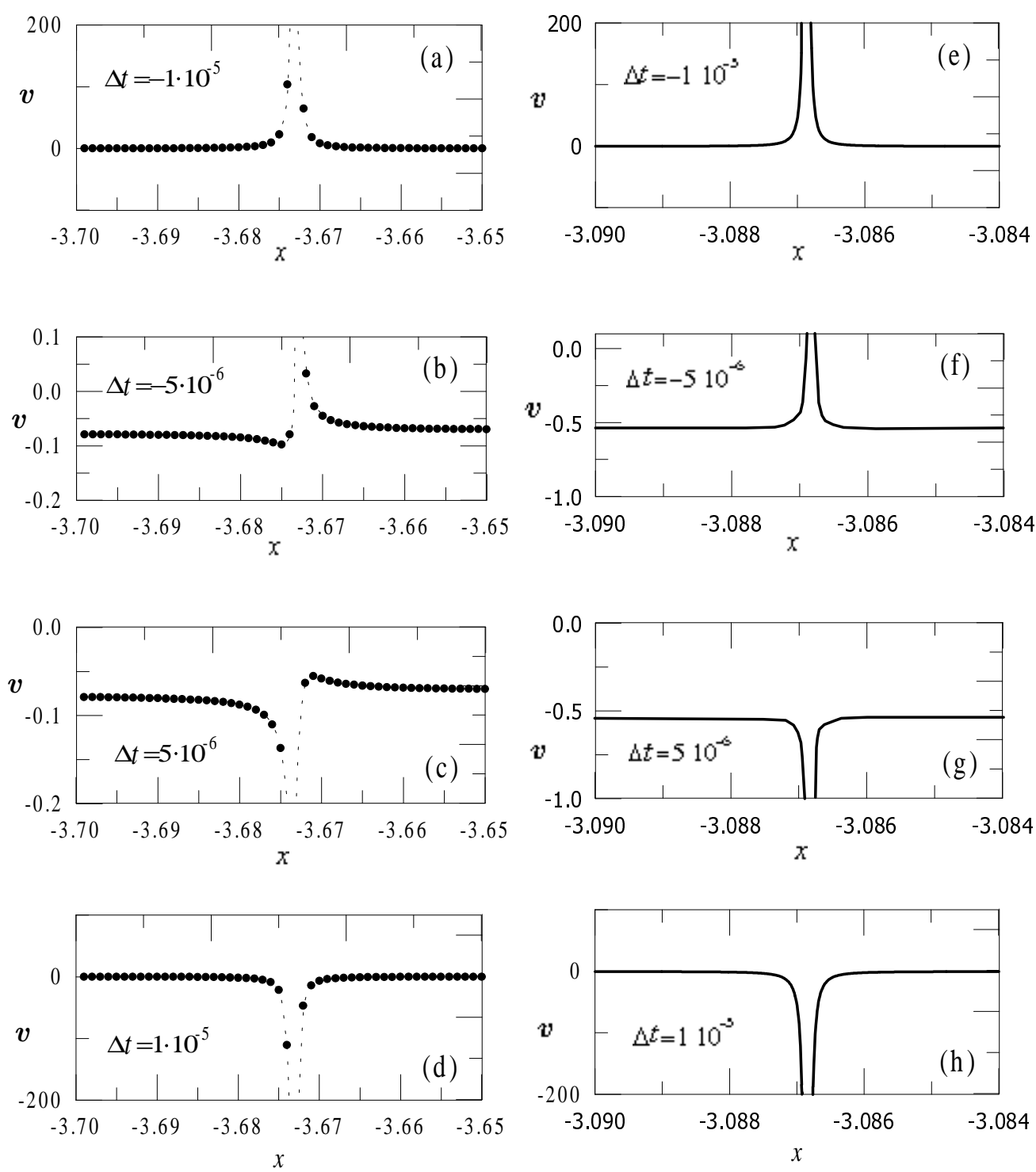


Fig.4

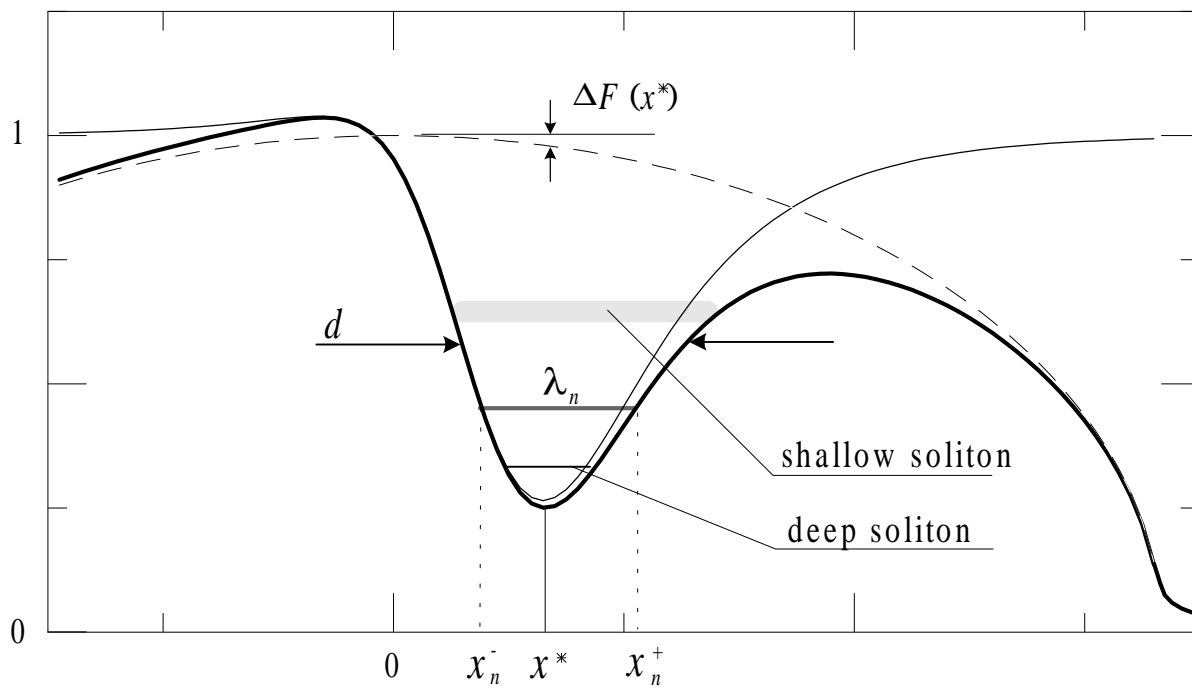


Fig.5

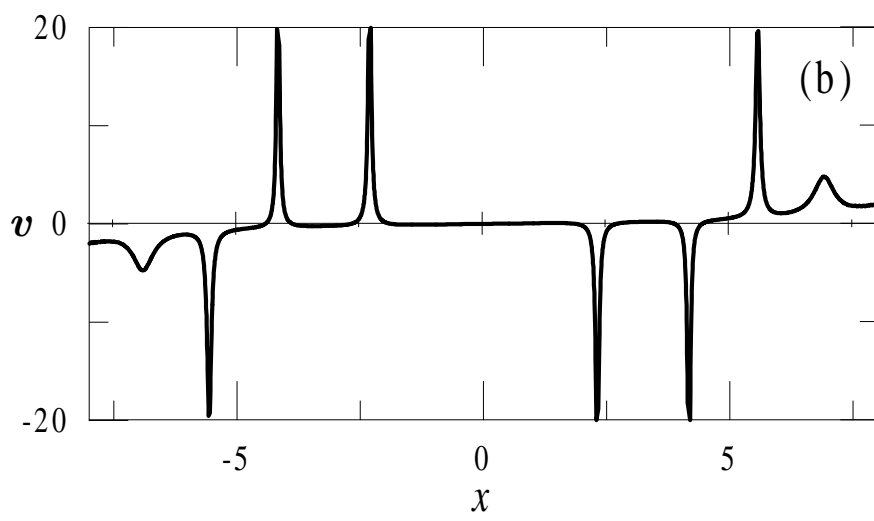
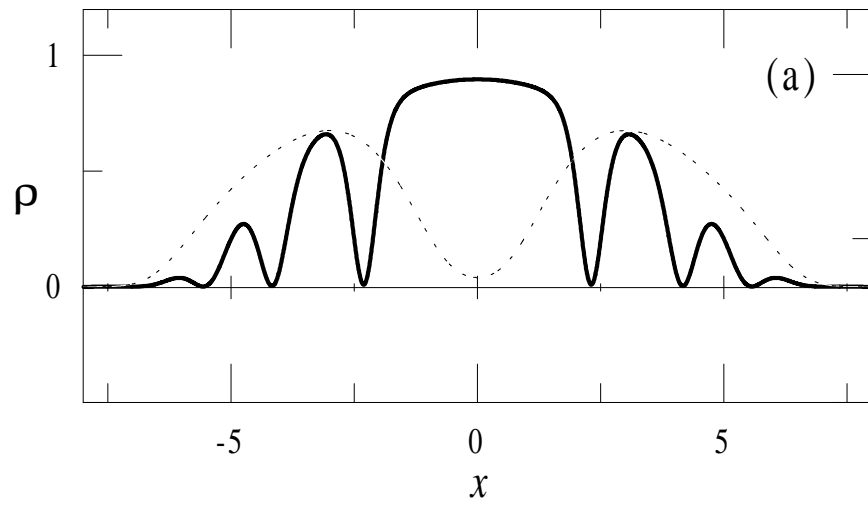


Fig.6

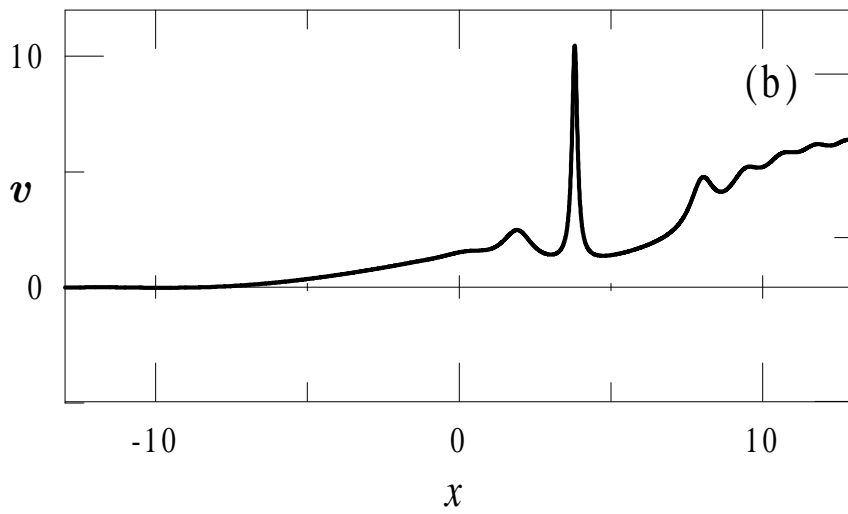
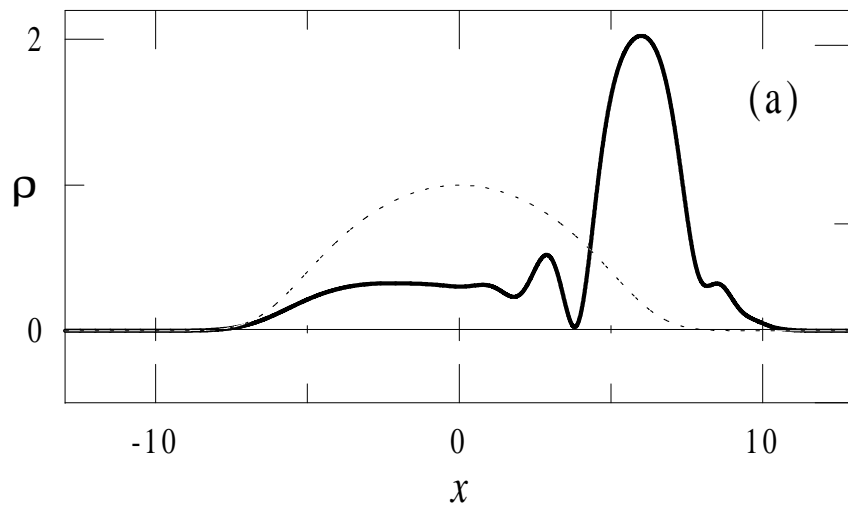


Fig.7

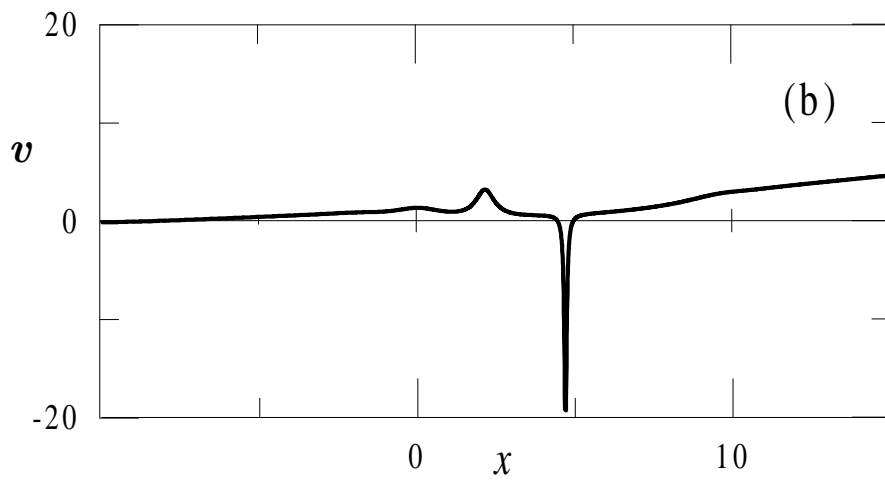
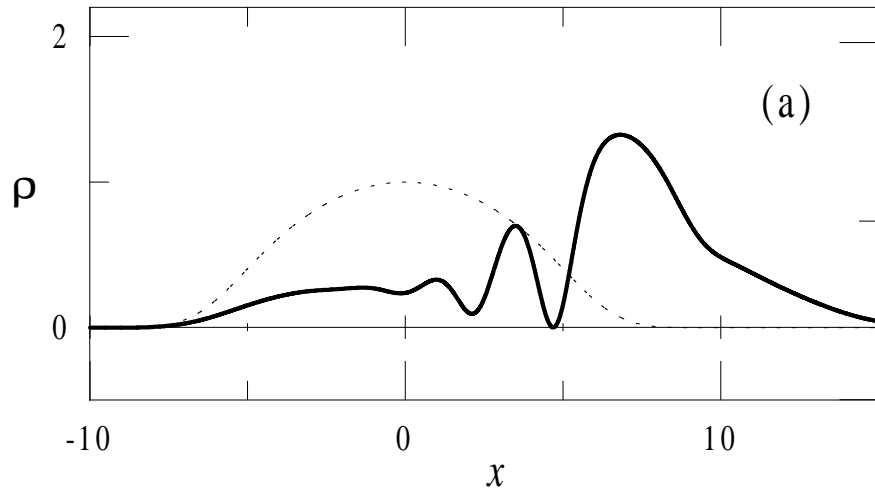


Fig.8

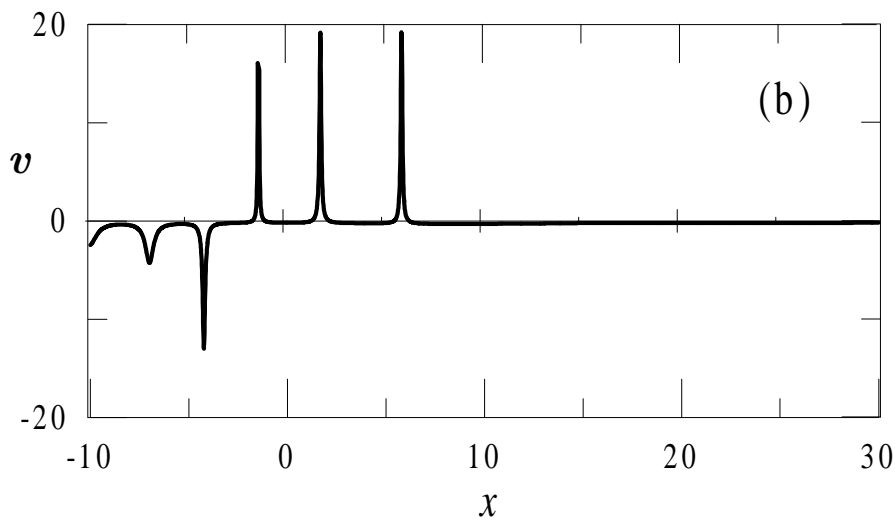
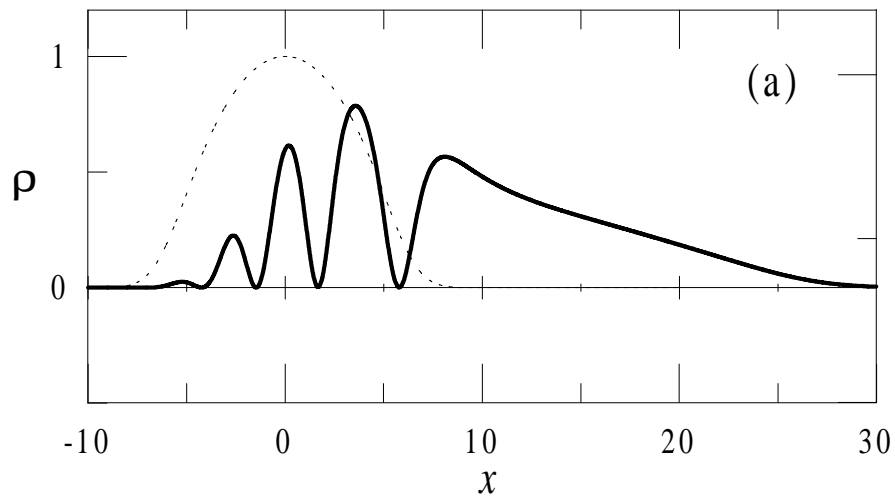


Fig.9

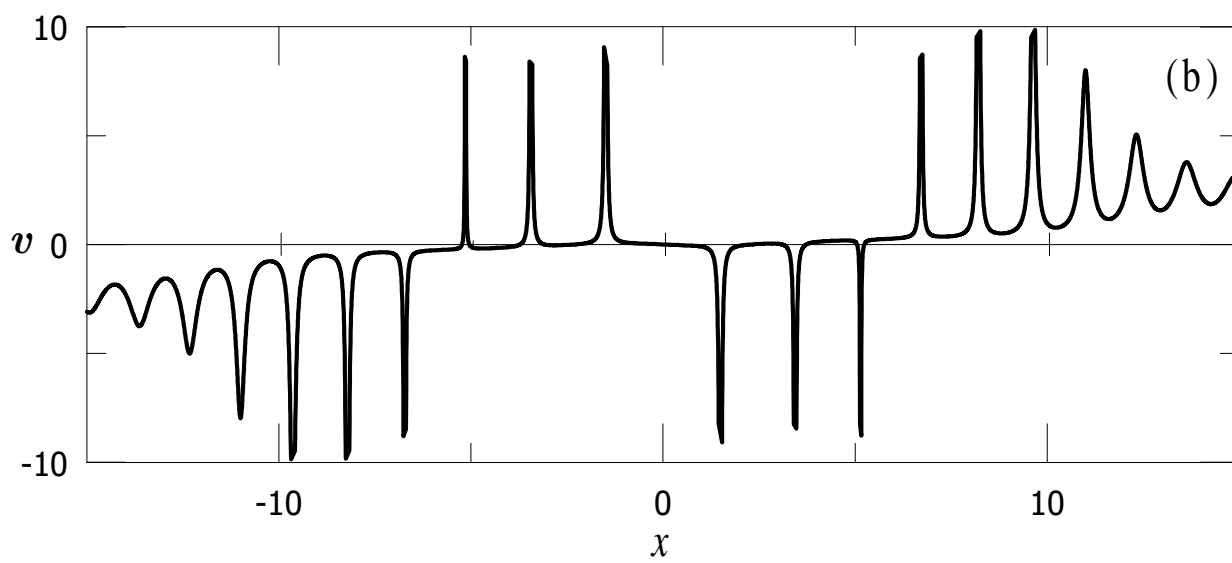
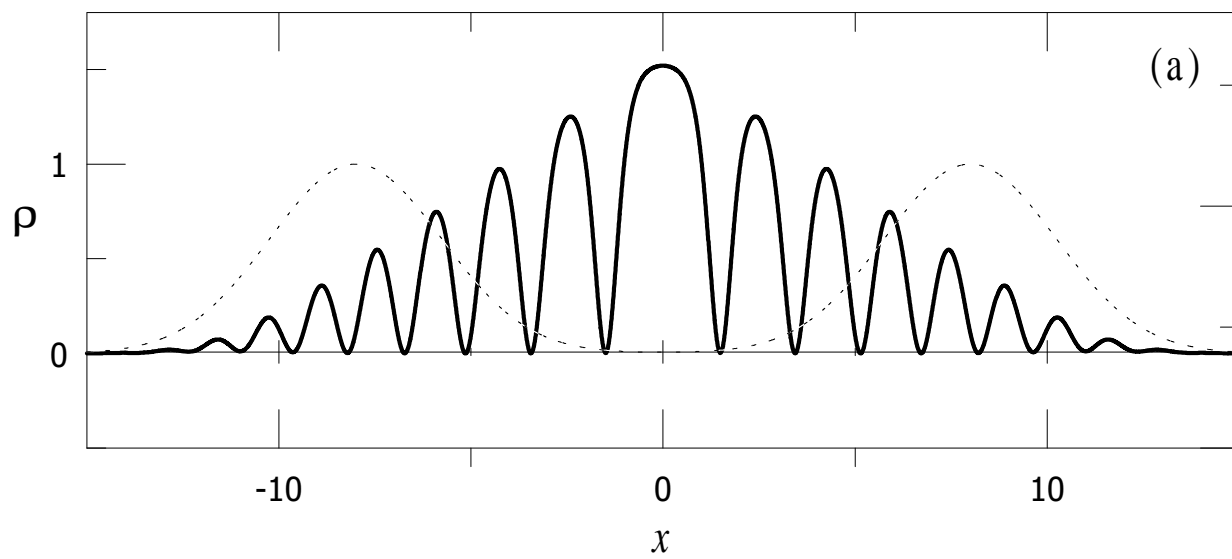


Fig.10